The Effects of Long Planetary Waves on the Regions of Cyclogenesis: Linear Theory

J. S. FREDERIKSEN

CSIRO Division of Atmospheric Physics, Aspendale, Victoria, Australia 3195

(Manuscript received 29 June 1978, in revised form 19 October 1978)

ABSTRACT

A study is made of the effect of a long planetary wave on the regions of preferential development, eddy momentum and heat fluxes, and the growth rates and phase speeds of growing baroclinic disturbances. The model used is a linear, spherical, two-layer quasi-geostrophic model with a basic state consisting of a 30° jet and an upper layer long planetary wave which together provide an approximate representation of the observed average Northern Hemisphere winter flow. The results of the baroclinic instability theory are compared with the observed regions of most actively developing baroclinic disturbances and eddy momentum and heat fluxes. Considering the crude vertical structure of two-layer models, the agreement between the theoretical and observed results is noteworthy. Details such as the observed latitudinal gaps between the jet-stream maxima and the regions of most actively developing eddies are reproduced in the model. Both these gaps and much of the horizontal variations of the theoretical and observed eddy momentum and heat fluxes are related to Phillips' criterion for incipient instability. Finally, closure hypotheses, needed for statistical dynamical models in which long waves as well as zonally averaged quantities are to be predicted, are proposed.

1. Introduction

The concept of long planetary waves steering short-wave cyclones and playing a major role in determining the regions of cyclogenesis (and anticyclogenesis) is quite old in meteorology. Baroclinic instability studies of atmospheric flows have, however, tended to concentrate on basic flows with no longitudinal (or time) variations [e.g., Baines and Frederiksen (1978) and references therein]. Recently, the stability of basic flows incorporating finite-amplitude long planetary waves was studied in two-layer quasi-geostrophic models on a sphere (Frederiksen, 1978a, hereafter denoted F). It was found that long planetary waves may have a considerable effect in modifying the growth rates, streamfunctions and *zonally averaged* eddy momentum and heat fluxes obtained using purely zonal flow profiles. Basic states consisting of a number of different stationary and transient long waves together with either solid body rotation or a 39° jet (characteristic of the zonally and yearly averaged observed Northern Hemisphere flow) were considered.

In this paper, a two-layer quasi-geostrophic spherical model is used to examine the stability of a basic profile consisting of a long zonal wavenumber 3 planetary wave and a winter jet; in particular, we study the regions of preferential cyclogenesis and the longitudinal variations of eddy heat and momentum fluxes. To the author's knowledge, the effects of long planetary waves on the longitudinal variations of eddy heat and momentum fluxes have not previously been studied within the context of baroclinic instability theory. These variations, however, are of considerable importance both for comparison with recent observational studies such as those of Blackmon *et al.* (1977) and for developing eddy flux parameterizations needed in statistical dynamical models where the long waves as well as zonally averaged quantities are predicted but the effects of short waves are parameterized. The desirability of developing such models will be discussed in detail in this paper.

In Section 2, the stability problem for basic flow profiles incorporating long planetary waves is formulated in the P model. The P model, introduced by Lorenz (1960), formally extends the quasi-geostrophic two-layer equations to the whole of the sphere. Section 3 defines the basic state which, to within the limitations of using a two-layer model incorporating a single planetary long wave, provides a reasonable approximation to the observed average Northern Hemisphere winter flow, as compiled from observations by Blackmon *et al.* (1977).

In Section 4, the growth rates and phase speeds of the growing disturbances are analyzed. The perturbation streamfunctions and the regions of preferential cyclogenesis are studied in Section 5, while in Section 6 the horizontal variations of the eddy heat and momentum fluxes are examined. In these latter

0022-4928/79/020195-10$06.50

two sections, we also compare our results with the observational studies of Blackmon (1976) and Blackmon *et al.* (1977); both theoretical and observed results are related to Phillips' (1954) criterion for incipient instability.

On the basis of the results in Sections 5 and 6, we propose, in Section 7, closure hypotheses needed for statistical dynamical models in which long waves as well as zonally averaged quantities are to be predicted but for which the effects of short waves are to be parameterized. The conclusions are summarized in Section 8 and details of the calculation of eddy momentum and heat fluxes are given in the Appendix.

2. Model details

The two-layer, spherical, quasi-geostrophic P model, derived by Lorenz (1960), has two layers centered at 750 and 250 mb, and the dimensionless forms of the equations, obtained by taking a (earth's radius) and Ω^{-1} (earth's angular velocity)$^{-1}$ as length and time scales and $a^2\Omega^2/bc_p$ as a temperature scale, are

$$\frac{\partial\theta}{\partial t}=-J(\psi,\theta)+\bar{\sigma}\nabla^2\chi, \tag{2.1a}$$

$$\frac{\partial\nabla^2\psi}{\partial t}=-J(\psi,\nabla^2\psi+2\mu)-J(\tau,\nabla^2\tau), \tag{2.1b}$$

$$\frac{\partial\nabla^2\tau}{\partial t}=-J(\psi,\nabla^2\tau)-J(\tau,\nabla^2\psi+2\mu)+\nabla\cdot 2\mu\nabla\chi, \tag{2.1c}$$

$$\nabla^2\theta=\nabla\cdot 2\mu\nabla\tau. \tag{2.1d}$$

In fact, since our basic states will include a planetary wave as well as zonal flow, it is necessary to depart from the idealized adiabatic frictionless equations and consider the more general equations which incorporate additional effects such as heating, topography and friction. These effects may be assumed to be incorporated by adding to the right-hand sides of Eqs. (2.1a), (2.1b) and (2.1c) additional terms which we denote F_θ, F_ψ and F_τ, respectively [cf. Eq. (3) of Baer and Alyea, 1971].

In the above equations,

$$b=\tfrac{1}{2}[(\tfrac{3}{4})^\kappa-(\tfrac{1}{4})^\kappa], \tag{2.2}$$

where $\kappa=R/c_p$, the ratio of the gas constant to the specific heat of air at constant pressure. Further, the streamfunctions in the upper (ψ^1) and lower (ψ^3) layers are related to the average ψ and shear τ streamfunctions through the relations

$$\psi=\tfrac{1}{2}(\psi^1+\psi^3),\quad \tau=\tfrac{1}{2}(\psi^1-\psi^3). \tag{2.3}$$

Here θ is the 500 mb potential temperature and χ the velocity potential in the lower layer. The static stability parameter $\bar{\sigma}$ measures the 250–750 mb potential temperature difference and $\mu=\sin\phi$, where ϕ is the latitude.

Rather than specifying F_θ, F_ψ and F_τ explicitly, we specify the basic state whose stability we shall study. For the basic states (denoted by a bar) we take streamfunctions consisting of a general zonal flow profile and a planetary wave:

$$\bar{\psi}^j=\bar{\psi}^j_0+\bar{\psi}^j_\rho,\quad j=1,3$$
$$=-A^j_{0N}P^0_N(\mu)-\mathrm{Re}[A^j_{\rho\nu}P^\rho_\nu(\mu)\exp i(\rho\lambda-\tilde{\omega}t)], \tag{2.4}$$

where summation over odd N up to an arbitrary odd $N_{\max}$ is implied. However, for the sake of simplicity, we restrict our consideration to a single planetary wave. Here $A^j_{\rho\nu}$ are amplitude coefficients, $P^\rho_\nu(\mu)$ are normalized Legendre functions [see Eq. (3.2) of Baines and Frederiksen, 1978], λ is the longitude, t the time, ρ the zonal wavenumber, ν the total wavenumber and $\tilde{\omega}$ the angular frequency.

With ψ^j given in Eq. (2.4), the relation (2.1d) then determines the functional form of θ [given in Eq. (A.1b) of F]. Further, the terms F_θ, F_ψ and F_τ are constrained to satisfy the prognostic equations with these functional forms of ψ^j and θ inserted. As in F, we neglect the effect of the forcing on the perturbations. As discussed there, this is in general quite a good approximation and is exact for completely inhomogeneous forcing (see also Charney, 1959).

In order to study the stability of the basic flow profile to small disturbances, Eq. (2.1) is linearized by replacing each field by a basic field (denoted by a bar) and a perturbation field (which for convenience is denoted by the original symbol). Only quantities which are first order in the perturbation fields are retained in the equations for the perturbation fields. We consider general disturbances of the form

$$f=\mathrm{Re}\{\sum_{n=1}^{\infty}\sum_{k=-n}^{n}f_{kn}P^k_n(\mu)\exp[i(k\lambda-\omega t)]\}, \tag{2.5}$$

where f is any of the fields in Eq. (2.1). The resultant eigenvalue-eigenvector equations for the complex angular frequency $\omega=\omega_r+i\omega_i$ and the amplitude coefficients f_{kn} are formulated in the Appendix of F.

3. The basic state

For the basic state whose stability we examine, we choose a profile which (to within the limitations of a two-layer model incorporating a single planetary wave in the basic profile) provides an approximate representation of the mean Northern Hemisphere winter charts. In the lower layer we assume no motion (in particular, no planetary wave), while in the upper layer, the purely zonal flow contribution is a 30° jet whose dimensional (nondivergent) velocity is

$$\bar{u}^1_0=-(1-\mu^2)^{\frac{1}{2}}\frac{\partial\bar{\psi}^1_0}{\partial\mu}a\Omega=40\sin^2\pi\mu\ [\mathrm{m\ s^{-1}}]. \tag{3.1}$$

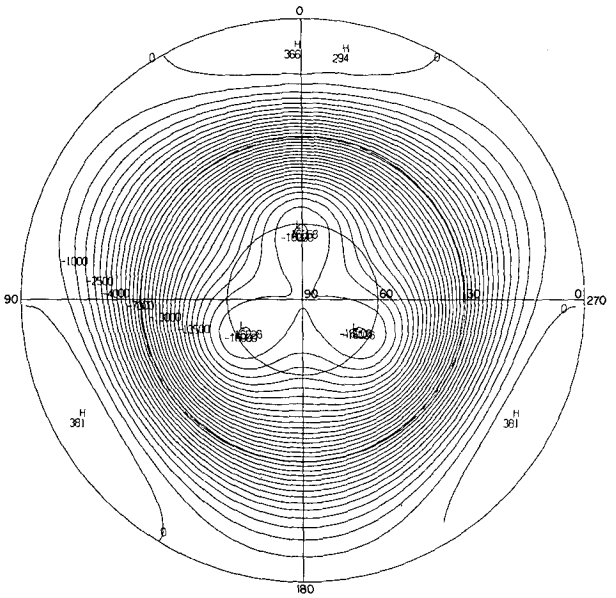

FIG. 1. Contour map of the (dimensional) streamfunction in the upper layer for the 30° jet together with the planetary wave P_6^3. The units shown correspond to 10^4 m^2 s^{-1}.

To obtain the purely zonal flow contribution to the basic streamfunction $\bar{\psi}_0^1$, the derivative $\partial\bar{\psi}_0^1/\partial\mu$ is expanded as an even (tenth degree) least-squares polynomial in μ; this is then reexpressed in terms of the derivatives of the normalized Legendre polynomials $\partial P_N^0(\mu)/\partial\mu$ to obtain all the nonzero A_{0N}^1 needed in Eq. (2.4). For the planetary wave contribution to the basic streamfunction in the upper layer we take a single stationary ($\tilde{\omega}=0$) wave with zonal wavenumber $\rho=3$ and total wavenumber $\nu=6(P_6^3)$ and amplitude coefficient

$$A_{36}^1=0.00334. \tag{3.2}$$

Fig. 1 shows the (dimensional) basic streamfunction in the upper layer for the 30° jet together with the planetary wave P_6^3. Notice that on rotating the coordinate system Fig. 1 resembles the mean Northern Hemisphere winter 500 mb *geopotential height* charts in Fig. 3.1 of Palmén and Newton (1969) and Fig. 3b of Blackmon (1976), except that in these charts the trough over Europe is somewhat weaker than those on the east coasts of America and Asia. Shown in Fig. 2 is the corresponding (dimensional) zonal velocity in the upper layer $\bar{u}^1$ when $\cos3\lambda=0, \pm1$ (or, since $\bar{u}^3=0$, the vertical shear $\bar{u}^1-\bar{u}^3$). Also shown are the contribution to the zonal velocity in the upper layer from the wave P_6^3 when $\cos3\lambda=1$, and Phillips' (1954) criterion for incipient instability for the P model:

$$|\bar{u}^1-\bar{u}^3|=\tilde{\sigma}a\Omega\cos\phi/\sin^2\phi. \tag{3.3}$$

As in F, we use a realistic atmospheric value of

$$\tilde{\sigma}=0.01 \tag{3.4}$$

for the static stability parameter.

We notice that the maximum value of $\bar{u}_0^1$ of 40 m s^{-1} at 250 mb corresponds closely to the mean January value of the Northern Hemisphere zonal wind of 39.8 m s^{-1} at 200 mb and 30°N as given in Table A8 of Oort and Rasmusson (1971). Further, the zonal wavenumber 3 structure and qualitative latitudinal variation of the zonal wind in Fig. 2 are quite similar to the corresponding quantities for the average winter 500 mb zonal wind in Fig. 6a of Blackmon *et al.* (1977). However, in their diagram, the jet maximum over the North Africa–Arabia region is considerably weaker than those off the east coasts of Asia and America.

Throughout the remainder of this article we shall, as in F, restrict our attention to the even perturbation modes (antisymmetric streamfunctions).

4. Growth rates and phase speeds

We show in Figs. 3a and 3b, respectively, the growth rates (ω_i) and phase speeds (ω_r/k) of the fastest growing even disturbance waves, as a function of zonal wavenumber k, for the 30° jet by itself. Also shown are the growth rate and phase speed of the fastest growing wave for the 30° jet together with the upper layer wave P_6^3, defined in Section 3. As in F, these spectra have been associated with a dominant zonal wavenumber $k^*=7$. The dominant

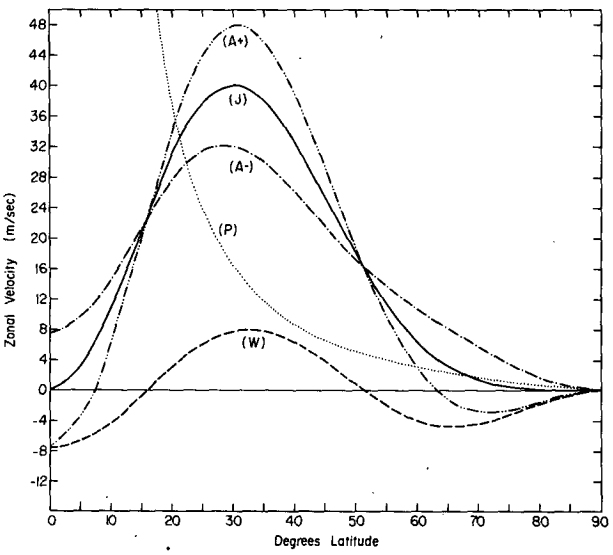

FIG. 2. The difference of the basic (dimensional) zonal velocities in the upper and lower layers $\bar{u}^1-\bar{u}^3$ for for 30° jet (J), for the wave P_6^3 when $\cos3\lambda=1$ [with amplitude coefficient given in Eq. (3.2)] (W), and for the 30° jet together with the wave P_6^3 when $\cos3\lambda=\pm1$, respectively (A±). Also shown is Phillips' stability criterion for the P model (P).

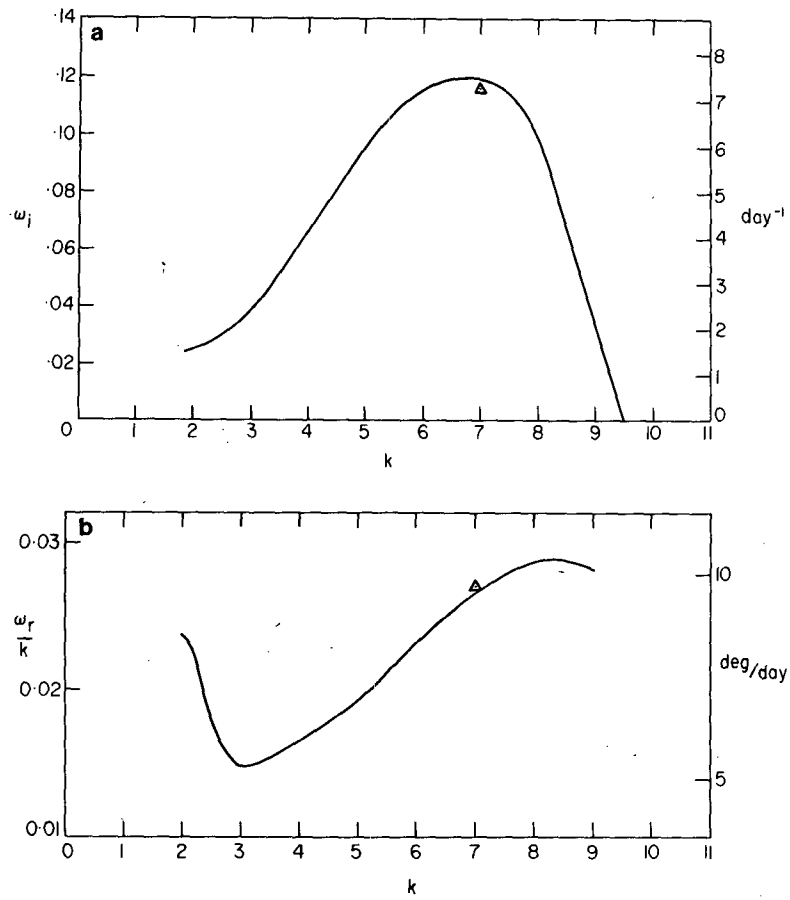

FIG. 3. Growth rates ω_i (a) and phase speeds ω_r/k (b) as a function of k for the fastest growing even disturbance modes for the 30° jet (solid line) and for the fastest growing mode with $k^*=7$ for the 30° jet together with the planetary wave P_6^3 (triangle).

zonal wavenumber k^* is defined as that wavenumber for which the contribution to the total energy of the perturbation is a maximum. For the P model, the total energy in a given zonal wavenumber k is given by

$$E(k)=\pi \sum_{n=|k|}^{\infty} n(n+1)[\psi_{kn}\psi^*_{kn}+\tau_{kn}\tau^*_{kn}]+\bar{\sigma}^{-1}\theta_{kn}\theta^*_{kn}. \quad (4.1)$$

As noted in F, the presence of a planetary wave with zonal wavenumber 3 causes a coupling of all the zonal wavenumbers of the perturbations which are related through addition of an integral multiple of 3. For the results in Figs. 3a and 3b, we retained in the expansion (2.5) zonal wavenumbers $k=1$, 4, 7, 10 and 13; the corresponding energies as a percentage of the energy in $k^*=7$ are, respectively, 0.27, 7.66, 100, 4.39 and 0.13%. Thus, the energy spectrum is strongly peaked at $k=7$. The total wavenumber n of the anti-symmetric disturbance streamfunctions take the values $n=k+1, k+3, \ldots, k+J$; we use $J=23$, which is sufficient to obtain convergence for the fastest growing mode. (Questions of convergence were discussed in more detail in F.)

From Fig. 3, it is evident that the presence of the upper layer long wave causes little change in the growth rate and phase speed spectra; this is consistent with the findings in F where, in comparison, pure barotropic and pure baroclinic waves were found to produce much larger changes in the growth rate spectra. Further, we note that at $k=7$ the growth rates and phase speeds in Fig. 3, for the 30° jet by itself (and with the long wave present), are quite similar to the eight-level results of Simmons and Hoskins (1976) and Frederiksen (1978b) for a similar jet.

The fastest growing mode (taken over all zonal wavenumbers) is commonly regarded as being of the most meteorological significance. For this reason, we concentrate throughout the remainder of this article on the fastest growing mode with $k^*=7$, for the basic state consisting of the 30° jet together with the upper layer wave P_6^3. As will be discussed in detail in a forthcoming article on baroclinic instability theory involving basic planetary waves and zonal flows in multi-level models (Frederiksen, 1979), the qualitative

bahaviors regarding the regions of preferential development, momentum and heat fluxes are in general very similar for the fastest growing modes with growth rates near the growth rate maximum.

5. Disturbance streamfunctions

Fig. 4 shows the disturbance streamfunction in the upper layer (at $t=0$) for the fastest growing mode with $k^*=7$, when the planetary wave P_6^3 is present in the basic state. The corresponding streamfunction in the lower layer is quite similar, but the maximum amplitude is somewhat smaller. Comparing Figs. 2 and 4, we see that the maximum development occurs slightly downstream of the positions where the excess shear [the difference between the vertical shear and Phillips' criterion (3.3)] is a maximum. This occurs when $\cos 3\lambda=1$, corresponding to the long-wave troughs of $-A_{36}^1 P_6^3(\mu)\, a^2\Omega\cos 3\lambda$ closest to the pole. Thus, the presence of the other zonal wavenumbers, particularly $k=4$ and 10 (and their conjugates), in the perturbation streamfunction causes a modulation of the zonal wavenumber 7 structure through a mechanism similar to beats, with the beat wavenumber being that of the basic wave, namely, 3.

We see from Fig. 4 that both regions of preferential cyclogenesis and anticyclogenesis occur downstream of the positions of maximum excess shear. Linear theories do not of course distinguish between the prevalence and intensity of highs and lows; in fact, because of the factor $\exp[-i(\omega_r+i\omega_i)t]$ in Eq. (2.5) these will be interchanged in the course of time.

It is interesting to compare Fig. 4 with Figs. 5a and 5c of Blackmon (1976) which show the winter band pass variance[1] of the observed 500 mb geopotential height field and indicate the regions of actively developing baroclinic disturbances. Recalling the similarity between our Fig. 2 and Fig. 6a of Blackmon *et al.* (1977) [apart from the weaker observed jet over North Africa–Arabia], we see that for both theoretical and observational results, the regions of the most actively developing disturbances occur slightly downstream and poleward of the positions of maximum zonal velocity. As might be expected from the fact that the jet over North Africa–Arabia is considerably weaker than those on the east coasts of America and Asia, there is no well-defined maximum in the band-pass variance over central Asia in Figs. 5a and 5c of Blackmon. Further, because of time averaging and incorporation of all (significant) zonal wavenumbers the wavenumber 7 structure is absent in these diagrams.

We note that while Blackmon *et al.* point out that

[1] The band-pass filter of Blackmon (1976) and Blackmon *et al.* (1977) is designed to retain fluctuations with periods between about 2.5 and 6 days. These band-pass fluctuations are found observationally to be associated with developing baroclinic waves.

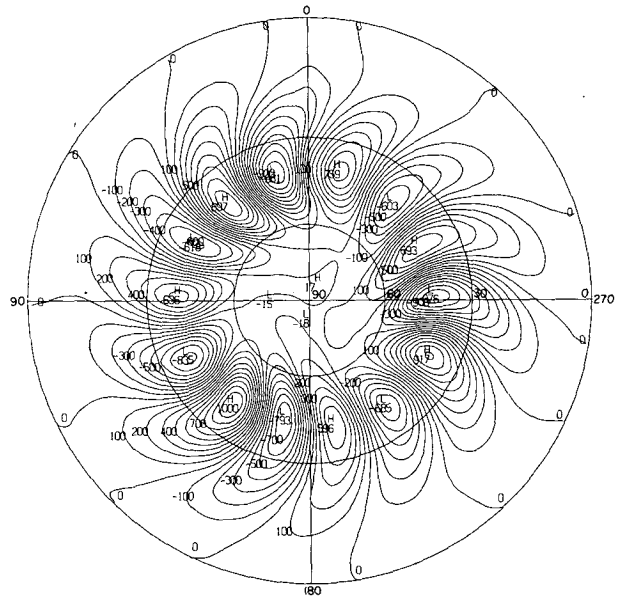

FIG. 4. Disturbance streamfunction ψ^1 in the upper layer (at $t=0$) for the fastest growing even mode with $k^*=7$ for a basic flow consisting of the 30° jet and the upper layer wave P_6^3.

there is a latitudinal gap between the jet maxima and the positions of the storm tracks, they are not certain whether this gap is significant. However, it would seem that this observation is a verification of the hypothesis in F that the positions of maximum development occur slightly downstream of the positions of maximum excess shear, which are poleward of the jet maxima, as seen from Fig. 2. We note from Tables A8 and A1 of Oort and Rasmusson that for January and, in fact, the whole winter period, both the 200–700 mb shear and the 500 mb zonal velocity have maxima at 30°N.

6. Momentum and heat fluxes

We now study the horizontal variations of the eddy momentum and heat fluxes associated with the growing disturbance of Section 5. The nondivergent eddy momentum flux (multiplied by $\cos^2\phi$) is defined by

$$u^j v^j(1-\mu^2)$$

$$=-(1-\mu^2)\frac{\partial\psi^j}{\partial\lambda}\frac{\partial\psi^j}{\partial\mu}, \quad j=1,3$$

$$=-(1-\mu^2)e^{2\omega_i t}\left(\frac{\partial\psi_+^j}{\partial\lambda}\frac{\partial\psi_-^j}{\partial\mu}+\frac{\partial\psi_-^j}{\partial\lambda}\frac{\partial\psi_+^j}{\partial\mu}\right)$$

$$-(1-\mu^2)e^{2\omega_i t}\left[\exp(-2i\omega_r t)\frac{\partial\psi_+^j}{\partial\lambda}\frac{\partial\psi_+^j}{\partial\mu}\right.$$

$$\left.+\exp(2i\omega_r t)\frac{\partial\psi_-^j}{\partial\lambda}\frac{\partial\psi_-^j}{\partial\mu}\right], \quad (6.1a)$$

where, since the perturbation streamfunctions of Section 5 do not involve the zonal wavenumber $k=0$,

$$\psi_+^j=\psi_-^{j*}=\sum_n\sum_{k\geq 1}\psi_{kn}^j P_n^k(\mu)e^{ik\lambda}. \tag{6.1b}$$

The nondivergent eddy potential temperature flux (multiplied by $\cos\phi$) is similarly defined by

$$\begin{aligned}&\tfrac{1}{2}\theta(v^1+v^3)(1-\mu^2)^{\frac{1}{2}}\\&=\tfrac{1}{2}\theta\left(\frac{\partial\psi^1}{\partial\lambda}+\frac{\partial\psi^3}{\partial\lambda}\right)\\&=e^{2\omega_i t}\left[\theta_+\left(\frac{\partial\psi_-^1}{\partial\lambda}+\frac{\partial\psi_-^3}{\partial\lambda}\right)+\theta_-\left(\frac{\partial\psi_+^1}{\partial\lambda}+\frac{\partial\psi_+^3}{\partial\lambda}\right)\right]\\&\quad+e^{2\omega_i t}\left[\exp(-2i\omega_r t)\theta_+\left(\frac{\partial\psi_+^1}{\partial\lambda}+\frac{\partial\psi_+^3}{\partial\lambda}\right)\right.\\&\qquad\left.+\exp(2i\omega_r t)\theta_-\left(\frac{\partial\psi_-^1}{\partial\lambda}+\frac{\partial\psi_-^3}{\partial\lambda}\right)\right],\end{aligned} \tag{6.2a}$$

where

$$\theta_+=\theta_-^*=\sum_n\sum_{k\geq 1}\theta_{kn}P_n^k(\mu)e^{ik\lambda}. \tag{6.2b}$$

The method of calculating these eddy fluxes is described in the Appendix.

Fig. 5 shows the eddy momentum flux in the upper layer $u^1v^1(1-\mu^2)$ at $t=0$, corresponding to the streamfunction in Fig. 4. The flux in the lower layer is similar but with a somewhat smaller maximum amplitude. Whereas for the 30° jet by itself the eddy momentum fluxes (not shown) have a periodic $k=14$ structure, here there is a strong modulation by the zonal wavenumber 3 of the basic wave. The fluxes have both poleward and equatorward components, producing maximum convergence of momentum slightly downstream of the positions of maximum excess shear. The fact that both poleward and equatorward fluxes occur may, generalizing the argument of Baines and Frederiksen (1978), be attributed to the fact that near 20° latitude the zonal flow profile changes from being stable to unstable according to Phillips' criterion while near 65°–70° latitude it changes from being unstable to stable again, with increasing latitude, for most longitudes.

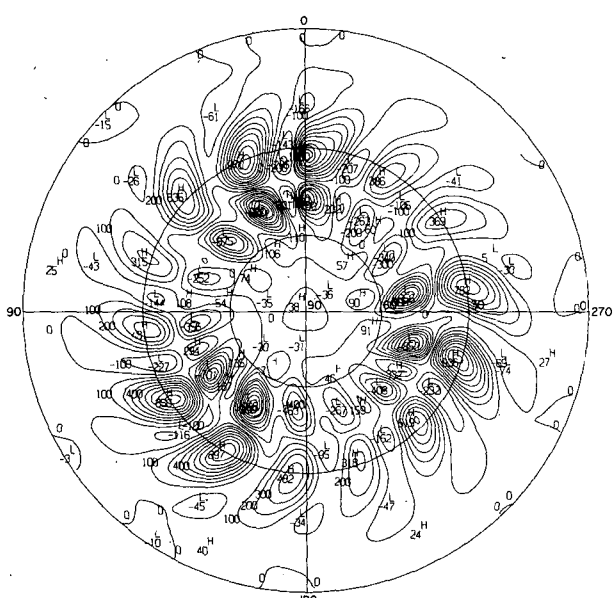

FIG. 5. Eddy momentum flux in the upper layer $u^1v^1(1-\mu^2)$ (at $t=0$) for the fastest growing even mode with $k^*=7$ and for the 30° jet and upper layer wave P_6^3. The normalization is 1000 arbitrary units.

From Eq. (6.1a), it may be seen that the momentum flux consists of an exponentially growing non-oscillatory component and a component which oscillates as well as grows. In view of the fact that observational studies such as those of Blackmon *et al.* involve time (and wavenumber) averaging, it seems more appropriate to compare the non-oscillatory component with such studies. Fig. 6 shows the non-oscillatory contribution to the momentum flux in the upper layer [divided by $\exp(2\omega_i t)$]. The $k=14$ structure has now been removed leaving mainly wavenumbers 3 and 0. We notice that downstream of the positions of maximum excess shear there are strong poleward and equatorward components with a maximum convergence of momentum while downstream of the positions of minimum excess shear the poleward flux is weak and there is practically no equatorward flux. We may therefore generalize the hypothesis of Baines and Frederiksen (1978): *At least to a first approximation, the direction of the non-oscillatory contribution to the momentum flux is poleward (respectively equatorward) slightly downstream of the regions where the basic zonal velocity profile changes from being stable to unstable (respectively unstable to stable) according to Phillips' criterion [Eq. (3.3)] with increasing latitude.*

Next, we compare Figs. 5 and 6 with the band-filtered momentum fluxes in Fig. 7b of Blackmon *et al.* We see that, apart from the region over North Africa–Arabia, where the observed jet maximum is considerably less than that used here, the regions of maximum convergence occur downstream of the position of maximum shear excess as in Fig. 6; further, for both our Fig. 6 and their Fig. 7b, the maximum poleward transports occur downstream of the jet maxima. We note, however [particularly because of the factor $(1-\mu^2)$ in Eq. (6.1a)], that our poleward fluxes are somewhat too small relative to the equatorward fluxes, compared with observations. This may be attributed to the differences in the profiles and the crudity of two-layer models. As discussed by Baines and Frederiksen (1978), momentum fluxes are very sensitive to small changes in the basic profiles. Nevertheless, the agreement between the observed and theoretical results, including the latitudinal gaps

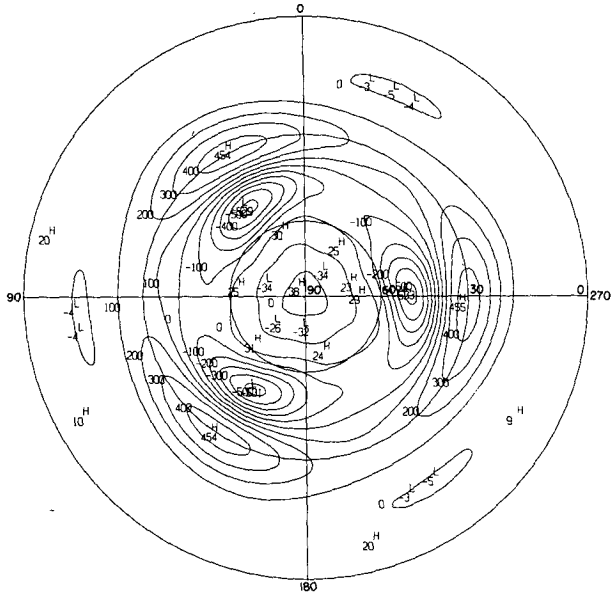

FIG. 6. The non-oscillatory (in time) contribution to the upper layer momentum flux $u^1v^1(1-\mu^2)$ [divided by $\exp 2\omega_i t$] for the fastest growing even mode with $k^*=7$ and for the 30° jet and upper layer wave P_6^3. The normalization is consistent with that in Fig. 5.

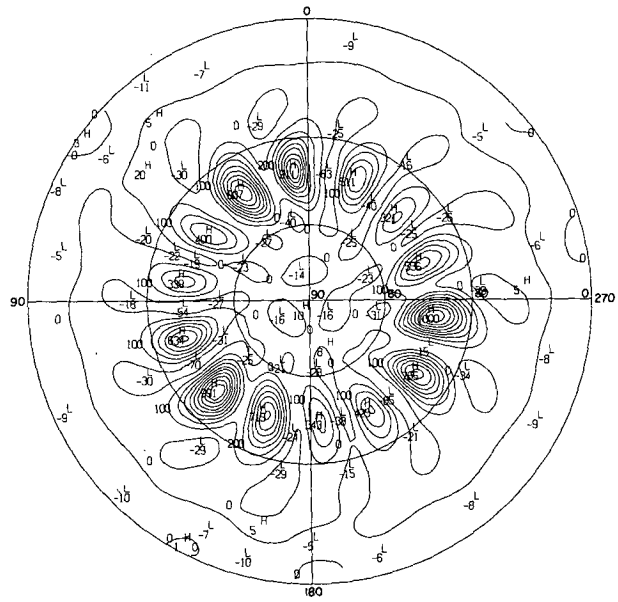

FIG. 7. As in Fig. 5 except for the eddy potential temperature flux $\frac{1}{2}\theta(v^1+v^3)(1-\mu^2)^{\frac{1}{2}}$ at $t=0$.

between the regions of maximum convergence and the jet maxima, is remarkable considering the simplicity of the model.

The model heat fluxes corresponding to the streamfunction in Fig. 4 are shown in Figs. 7 and 8. Fig. 7 shows the potential temperature flux $\frac{1}{2}\theta(v^1+v^3)(1-\mu^2)^{\frac{1}{2}}$ at $t=0$, while Fig. 8 shows the non-oscillatory contribution to this flux at any particular time (divided by $e^{2\omega_i t}$). In the former diagram there is again a strong modulation of the $k=14$ structure by the zonal wavenumber 3 while in the latter the $k=14$ structure has been removed leaving largely wavenumbers 3 and 0. In both cases, the maximum poleward flux occurs slightly downstream of the positions of maximum excess shear ($\cos 3\lambda=1$). Fig. 8 compares favorably with the observed band-pass transient eddy heat flux in Fig. 11b of Blackmon *et al.*, where the maximum poleward flux also occurs downstream and slightly poleward of the jet maxima (excluding again the region over central Asia). As discussed by Baines and Frederiksen (1978), heat fluxes are much less sensitive than momentum fluxes to small changes in model parameters.

While the horizontal variations of the non-oscillatory heat and momentum fluxes are in quite good agreement with observations, the ratio of the momentum to heat flux is underestimated by linear theory, as will be discussed in the following section.

7. Statistical dynamical models

It would seem, on the basis of the comparison of observed and theoretical fluxes discussed in Section 6, that linear theory may be able to provide closure hypotheses needed for statistical dynamical models in which long planetary waves as well as zonally averaged quantities are predicted. As far as zonally averaged statistical dynamical models are concerned, parameterizations of eddy fluxes based on baroclinic instability theories have been proposed by a number of authors; a review of these studies has been made by Schneider and Dickinson (1974; see also White, 1977). In these studies the latitudinal variations and

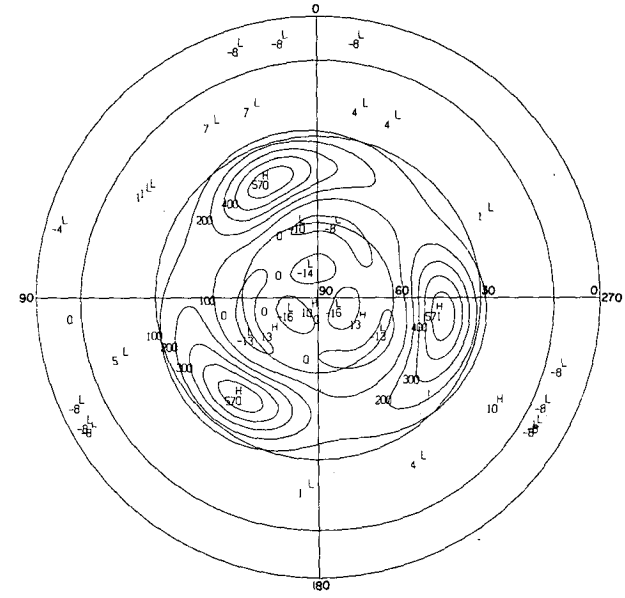

FIG. 8. As in Fig. 6 except for the eddy potential temperature flux $\frac{1}{2}\theta(v^1+v^3)(1-\mu^2)^{\frac{1}{2}}$ [divided by $\exp 2\omega_i t$].

relative magnitudes of the various parameterized fluxes are usually obtained (directly or indirectly) from the fastest growing modes (zonal wavenumbers 5–8) in baroclinic instability studies with purely zonal flow basic profiles. The absolute magnitudes of the fluxes are then obtained through heuristic (energy) arguments. However, it is well known that there is a basic distinction between the quasi-stationary long waves (zonal wavenumbers 1–4) which are forced by zonal variations in heating and topography and the transient baroclinic waves (zonal wavenumbers 5–8) which arise through instability. Further, the long waves contribute significantly to both heat and momentum fluxes (see, e.g., Oort and Rasmusson, 1971), and one should not expect to be able to parameterize these fluxes in terms of transient shorter wave baroclinic eddies. Thus, it would seem desirable to develop statistical dynamical models in which the long waves as well as zonally averaged quantities are predicted explicitly.

In order to illustrate a plausibility argument for determining flux parameterizations needed for statistical dynamical models incorporating long waves explicitly, we consider the primitive equation for the zonal velocity. In pressure coordinates, the (dimensional) equation is

$$\frac{\partial U}{\partial t}+\frac{1}{a(1-\mu^2)}\frac{\partial U^2}{\partial \lambda}+\frac{1}{a}\frac{\partial}{\partial \mu}UV+\frac{\partial}{\partial p}\omega U - 2\Omega\mu V+\frac{1}{a}\frac{\partial \Phi}{\partial \lambda}=0, \quad (7.1)$$

where U is the zonal velocity [$\times\cos\phi$], V the meridional velocity [$\times\cos\phi$], $\omega=dp/dt$ and Φ the geopotential height.

We now split each of the fields F in Eq. (7.1) into a quasi-stationary long wave and zonal flow component F^W and a remainder, which we denote the "perturbation" F', i.e.,

$$F=F^W+F'. \quad (7.2)$$

The quasi-stationary contributions are defined by

$$F^W=\sum_{\rho=0}^{R} F_\rho^W(t,\mu)e^{i\rho\lambda}+\text{cc}, \quad (7.3a)$$

where the time averaged Fourier coefficients are defined by

$$F_\rho^W(t,\mu)=\overline{\langle F\rangle^\rho}, \quad (7.3b)$$

cc denotes the complex conjugate and the most obvious choice for R is 4 as discussed above. The time averaging and Fourier projection operators needed in Eq. (7.3b) are defined by

$$\bar{F}=(1/2\Delta t)\int_{t-\Delta t}^{t+\Delta t} F dt', \quad (7.4a)$$

$$\langle F\rangle^\rho=(1/2\pi)\int_0^{2\pi} d\lambda e^{-i\rho\lambda}F, \quad (7.4b)$$

where the time interval of averaging Δt has yet to be specified. Similarly, with

$$\hat{F}\equiv F-\bar{F}, \quad (7.5a)$$

$$F'=\sum_{\rho=0}^{\infty} F'_\rho(t,\mu)e^{i\rho\lambda}+\text{cc}, \quad (7.5b)$$

where

$$F'_\rho(t,\mu)=\begin{cases}\langle\hat{F}\rangle^\rho & \text{for } \rho=0,1,\ldots,R \quad (7.5c)\\ \langle F\rangle^\rho & \text{for } \rho=R+1,\ldots,\infty. \quad (7.5d)\end{cases}$$

Equations for the complex Fourier coefficients $U_\rho^W(t,\mu)$, $\rho=0, 1, \ldots, R$, for the quasi-stationary long waves and zonal flow may then be obtained by operating on (7.1) with the Fourier projection and time averaging operators in (7.4). These equations also involve the "perturbation" fields F' both linearly in products like $a^{-1}\partial\overline{\langle U'V'^W\rangle^\rho}/\partial\mu$ and nonlinearly in terms like $a^{-1}\partial\overline{\langle U'V'\rangle^\rho}/\partial\mu$. We now make the following closure hypotheses:

(i) The time-averaged, Fourier projected products involving the "perturbation" fields linearly vanish, for all $\rho=0, 1, \ldots, R$.

(ii) The time-averaged, Fourier projected eddy fluxes are given (up to an arbitrary constant) by the Fourier projection of the non-oscillatory (in time) contribution to the corresponding fluxes obtained from the fastest growing modes in baroclinic instability theory. It is of course assumed in (ii) that the same equations are used in the baroclinic instability study as in the nonlinear model and that the basic state is determined by the statistical dynamical model at the previous time step. As in the usual zonally averaged models, the absolute magnitude of at least one of the fluxes must be obtained through heuristic energy arguments. Ideally, the relative magnitudes of the various fluxes should also be as determined from baroclinic instability theory. However, as discussed by Simmons and Hoskins (1977, 1978) and Gall (1976), for purely zonal flow basic states in linear multi-level models, the ratio of the eddy momentum to heat flux is smaller than observed. Thus, it may also be necessary when basic planetary waves are present to determine the magnitudes of the different fluxes empirically and independently. The vertical structure of the present two-layer model is probably too crude to attempt to decide this question in general. However, we note that the ratio of the maximum

poleward 250 mb non-oscillatory momentum flux $u^1v^1(1-\mu^2)a^2\Omega^2$ to the corresponding poleward 500 mb potential temperature flux $\frac{1}{2}(v^1+v^3)\theta(1-\mu^2)^{\frac{1}{2}}a^3\Omega^3/bc_p$ of Section 6 is 0.8 m s^{-1} K^{-1}. On the basis of the results of Blackmon *et al.* (1977) and Oort and Rasmusson (1971) for winter (suitably interpolated) it is estimated that the corresponding ratio of observed fluxes is some six or more times larger.

With the above assumptions the equations for $U_\rho^W(t,\mu)$ are

$$\frac{\delta U^W}{\delta t}+\frac{1}{a(1-\mu^2)}\left[\left\langle\frac{\partial U^{W2}}{\partial\lambda}\right\rangle^\rho+\left\langle\frac{\partial U'^2}{\partial\lambda}\right\rangle^\rho\right]$$
$$+\frac{1}{a}\left[\frac{\partial}{\partial\mu}\langle U^W V^W\rangle^\rho+\frac{\partial}{\partial\mu}\langle U'V'\rangle^\rho\right]$$
$$+\left[\frac{\partial}{\partial p}\overline{\langle\omega^W U^W\rangle^\rho}+\frac{\partial}{\partial p}\overline{\langle\omega' U'\rangle^\rho}\right]-2\Omega\mu V_\rho^W$$
$$+\frac{1}{a}\left\langle\overline{\frac{\partial\phi^W}{\partial\lambda}}\right\rangle^\rho=0, \quad (7.6a)$$

where $\rho=0, 1, \ldots, R$ and

$$\frac{\delta U_\rho^W}{\delta t}\equiv\frac{U_\rho^W(t+\Delta t,\mu)-U_\rho^W(t-\Delta t,\mu)}{2\Delta t}. \quad (7.6b)$$

Similar equations may be derived for the meridional velocity and the temperature, for which the hypotheses (i) and (ii) are also assumed to apply.

Assumptions (i) and (ii) seem plausible in that, taking $R=4$, the "perturbation" fields correspond to transient waves with a short time scale in comparison with the quasi-stationary long waves; we see from Eq. (7.5c) that the long-wave contribution to the "perturbations" are explicitly transient, while observationally it is found that the short waves are transient. From the point of view of linear stability theory, the assumptions correspond to neglecting all terms that oscillate in time. We also see that the usual temporal finite-difference equations for zonally averaged models may be recovered by taking $R=0$ and approximating the time-averaged quasi-stationary terms by their values at t. For zonally averaged models hypotheses (i) and (ii) are, of course, valid without time averaging since zonal averaging removes terms linear in the "perturbation" fields and as well removes the oscillatory time dependence in the eddy fluxes through selecting only the zonal wavenumber 0 contribution which is non-oscillatory. Most importantly, however, hypothesis (ii) appears to be consistent with observational data on eddy fluxes as discussed in Section 6. The time interval Δt which may be used remains a matter for experimentation; however, depending of course on the meridional resolution, it would seem that this may be increased considerably on the present approximately 1 h time step used in high-resolution general circulation models with semi-implicit algorithms.

8. Conclusions

The effect of a finite-amplitude long planetary wave in changing growth rate and phase speed spectra, perturbation streamfunctions and eddy momentum and heat fluxes from the corresponding quantities obtained using a purely zonal flow 30° jet has been studied in a spherical linear two-layer quasi-geostrophic model. The 30° jet together with the upper layer wave (P_6^3) provide at least an approximate representation of some of the characteristics of the average Northern Hemisphere winter flow as determined by Blackmon *et al.* (1977).

The upper layer long wave is found to have little effect on the growth rate and phase speed of the fastest growing disturbance mode; however, it plays an important role in producing regions of preferential development downstream of the long-wave troughs closest to the pole. Moreover, it produces considerable changes in the horizontal variations of eddy momentum and heat fluxes. The regions of preferential development are found to compare favorably with the observed regions of actively developing baroclinic disturbances described by Blackmon (1976). Further, the agreement between the theoretical and observed time averaged eddy momentum and heat fluxes of Blackmon *et al.* (1977) is quite reasonable and is improved by comparing the latter with the non-oscillatory (in time) contribution to these fluxes. Both theoretical and observed regions of actively developing baroclinic disturbances and eddy momentum and heat fluxes are related to Phillips' (1954) criterion for incipient instability.

Our theoretical results are consistent with the heuristic model of the major winter jet streams proposed by Blackmon *et al.* (see also Namias and Clapp, 1949). They also suggest that the latitudinal gaps between the jet stream maxima and the storm tracks, as discussed by these authors, are, in fact, significant and are related to Phillips' criterion.

On the basis of the general agreement between observed and linear results, closure hypotheses, needed for statistical dynamical models in which the long planetary waves as well as zonally averaged quantities are predicted but the effects of the short waves are to be parameterized, have been proposed.

We conclude that much of the observed horizontal variation of the regions of active development and eddy momentum and heat fluxes may be explained on the basis of linear theory. The vertical variations of these quantities will be studied in multi-level models in future articles.

Acknowledgment. It is a pleasure to thank R. A. Plumb for an informative discussion.

APPENDIX

Calculation of Eddy Momentum and Heat Fluxes

The eddy momentum and heat fluxes at $t=0$ may be calculated as follows. The momentum fluxes are defined in Eq. (6.1), where the perturbation streamfunctions are given by the form (2.5) with $t=0$. Alternatively, the momentum fluxes may be expanded directly in terms of spherical harmonics, i.e.,

$$u^j v^j(1-\mu^2)=\sum_{n=1}^{\infty}\sum_{k=-n}^{n} M_{kn}^j P_n^k(\mu)e^{ik\lambda}, \quad j=1,3. \quad \text{(A1)}$$

Now on integrating both Eqs. (A1) and (6.1) over the surface of a sphere with weight function $P_n^k(\mu)e^{-ik\lambda}$ we find that, with the selection rule,

$$k=a+b, \quad \text{(A2a)}$$

$$M_{kn}^j=-i\sum_{\alpha}\sum_{a}\sum_{\beta}\sum_{b}\psi_{b\beta}^j\psi_{a\alpha}^j \times b[(\alpha+1)\epsilon_\alpha^a C_{n\ \beta\ \alpha-1}^{k\ b\ a}-\alpha\epsilon_{\alpha+1}^a C_{n\ \beta\ \alpha+1}^{k\ b\ a}]. \quad \text{(A2b)}$$

Here we have used the fact that

$$(1-\mu^2)\frac{\partial P_\alpha^a}{\partial\mu}=(\alpha+1)\epsilon_\alpha^a P_{\alpha-1}^a-\alpha\epsilon_{\alpha+1}^a P_{\alpha+1}^a, \quad \text{(A3)}$$

where

$$\epsilon_\alpha^a=[(\alpha^2-a^2)/(4\alpha^2-1)]^{\frac{1}{2}} \quad \text{(A4)}$$

and, in Eq. (A2),

$$C_{n\ \beta\ \alpha}^{k\ b\ a}=\int_{-1}^{1} d\mu P_n^k P_\beta^b P_\alpha^a. \quad \text{(A5)}$$

The integral (A5) vanishes unless the following selection rules are satisfied:

$$n+\beta+\alpha=\text{even integer}, \quad \text{(A6a)}$$

$$|\beta-\alpha|\leqslant n\leqslant\beta+\alpha. \quad \text{(A6b)}$$

Eq. (A5) defines the well-known angular momentum coupling integral of quantum mechanics (Edmonds, 1957) and may be evaluated using the formula of Racah (1942) (see also, Silberman, 1954 and Ellsaesser, 1966). Thus, the momentum fluxes may be calculated using Eqs. (A1)–(A6).

In a similar way, the potential temperature flux at $t=0$ is given by

$$\tfrac{1}{2}\theta(v^1+v^3)(1-\mu^2)^{\frac{1}{2}}=\sum_{k=1}^{\infty}\sum_{k=-n}^{n} H_{kn}P_n^k(\mu)e^{ik\lambda}, \quad \text{(A7)}$$

where, with the selection rules (A2a) and (A6),

$$H_{kn}=\tfrac{1}{2}i\sum_{\alpha}\sum_{a}\sum_{\beta}\sum_{b}\theta_{a\alpha}(\psi_{b\beta}^1+\psi_{b\beta}^3)bC_{n\ \beta\ \alpha}^{k\ b\ a}. \quad \text{(A8)}$$

Here we have used Eq. (6.2).

The non-oscillatory (in time) contributions to the momentum and heat fluxes discussed in Section 6 may be calculated in a similar way.

REFERENCES

Baer, F., and F. N. Alyea, 1971: Effects of spectral truncation on general circulation and long range prediction. *J. Atmos. Sci.*, **28**, 457–480.

Baines, P. G., and J. S. Frederiksen, 1978: Baroclinic instability on a sphere in two-layer models. *Quart. J. Roy. Meteor. Soc.*, **104**, 45–68.

Blackmon, M. L., 1976: A climatological spectral study of the 500 mb geopotential height of the Northern Hemisphere. *J. Atmos. Sci.*, **33**, 1607–1623.

——, J. M. Wallace, N. Lau and S. L. Mullen, 1977: An observational study of the Northern Hemisphere wintertime circulation. *J. Atmos. Sci.*, **34**, 1040–1053.

Charney, J. G., 1959: On the general circulation of the atmosphere. *The Atmosphere and the Sea in Motion*, B. Bolin, Ed., Rockefeller Institute Press, 178–193.

Edmonds, A. R., 1957: *Angular Momentum in Qunatum Mechanics*. Princeton University Press, 140 pp.

Ellsaesser, H. W., 1966: Evaluation of spectral versus grid methods of hemispheric numerical weather prediction. *J. Appl. Meteor.*, **5**, 246–262.

Frederiksen, J. S., 1978a: Instability of planetary waves and zonal flows in two-layer models on a sphere. *Quart. J. Roy. Meteor. Soc.*, **104**, 841–872.

——, 1978b: Growth rates and phase speeds of baroclinic waves in multi-level models on a sphere. *J. Atmos. Sci.*, **35**, 1816–1826.

——, 1979: Baroclinic instability of zonal flows and planetary waves in multi-level models on a sphere. In preparation.

Gall, R., 1976: A comparison of linear baroclinic instability theory with the eddy statistics of a general circulation model. *J. Atmos. Sci.*, **33**, 349–373.

Lorenz, E. N., 1960: Energy and numerical weather prediction. *Tellus*, **12**, 364–373.

Namias, J., and P. F. Clapp, 1949: Confluence theory of the high tropospheric jet stream. *J. Meteor.*, **6**, 330–336.

Oort, A. H., and E. M. Rasmusson, 1971: *Atmospheric Circulation Statistics*. NOAA Prof. Pap. 5, 323 pp. [Govt. Printing Office, Stock no. 0317-0045, C55.25:5].

Palmén, E., and C. W. Newton, 1969: *Atmospheric Circulation Systems*. Academic Press, 603 pp.

Phillips, N. A., 1954: Energy transformations and meridional circulations associated with simple baroclinic waves in a two-level, quasi-geostrophic model. *Tellus*, **6**, 273–286.

Racah, G., 1942: Theory of complex spectra. II. *Phys. Rev.*, **62**, 438–462.

Schneider, S. H., and R. E. Dickinson, 1974: Climate modelling. *Rev. Geophys. Space Phys.*, **12**, 447–493.

Silberman, I., 1954: Planetary waves in the atmosphere. *J. Meteor.*, **11**, 27–34.

Simmons, A. J., and B. J. Hoskins, 1976: Baroclinic instability on the sphere: normal modes of the primitive and quasi-geostrophic equations. *J. Atmos. Sci.*, **33**, 1454–1477.

——, and ——, 1977: Baroclinic instability on the sphere: solutions with a more realistic tropopause. *J. Atmos. Sci.*, **34**, 581–588.

——, and ——, 1978: The life cycles of some nonlinear baroclinic waves. *J. Atmos. Sci.*, **35**, 414–432.

White, A. A., 1977: The surface flow in a statistical climate model—a test of a parameterization of large-scale momentum fluxes. *Quart. J. Roy. Meteor. Soc.*, **103**, 93–119.